Microfluidic Affinity Profiling reveals a Broad Range of Target Affinities for Anti-SARS-CoV-2 Antibodies in Plasma of Covid Survivors

Matthias M. Schneider[1,#], Marc Emmenegger[2,#], Catherine K. Xu[1,#], Itzel Condado Morales[2,#], Priscilla Turelli[3], Manuela R. Zimmermann[1], Beat M. Frey[4], Sebastian Fiedler[5], Viola Denninger[5], Georg Meisl[1], Vasilis Kosmoliaptsis[6,7], Heike Fiegler[5], Didier Trono[3], Tuomas P. J. Knowles[1,8*] , and Adriano Aguzzi[2*]

[1] Centre for Misfolding Diseases, Department of Chemistry, University of Cambridge, Lensfield Road, Cambridge CB2 1EW, United Kingdom

[2] Institute of Neuropathology, University of Zurich, 8091 Zurich, Switzerland

[3] School of Life Sciences, École Polytechnique Fédérale de Lausanne, Lausanne, Switzerland

[4] Regional Blood Transfusion Service Zurich, Swiss Red Cross, 8952 Schlieren, Switzerland

[5] Fluidic Analytics, Unit A, The Paddocks Business Centre, Cherry Hinton Rd, Cambridge CB1 8DH, UK

[6] Department of Surgery, Addenbrooke's Hospital, University of Cambridge, Hills Road, Cambridge CB2 0QQ, United Kingdom

[7] NIHR Blood and Transplant Research Unit in Organ Donation and Transplantation, University of Cambridge, Hills Road, Cambridge CB2 0QQ, United Kingdom

[8] Cavendish Laboratory, Department of Physics, University of Cambridge, JJ Thomson Ave, Cambridge CB3 0HE, United Kingdom

[#] equal contribution

*to whom correspondence should be addressed: adriano.aguzzi@usz.ch or tpjk2@cam.ac.uk

Abstract

The clinical outcome of SARS-CoV-2 infections can range from asymptomatic to lethal, and is thought to be crucially shaped by the quality of the immune response which includes antibody titres and affinity for their targets. Using Microfluidic Antibody Affinity Profiling (MAAP), we determined the aggregate affinities and concentrations of anti-SARS-CoV-2 antibodies in plasma samples of 42 seropositive individuals, 23 of whom were confirmed to be SARS-CoV-2-positive by PCR testing. We found that dissociation constants (K_d) of anti-RBD antibodies spanned more than two orders of magnitude from 80 pM to 25 nM, despite having similar antibody concentrations. The tested individuals showed progressively higher antibody concentrations but constant K_d values, suggesting that affinities did not mature over time. 33 sera showed affinities higher than that of the CoV2 spike for its ACE2 receptor. Accordingly, addition of seropositive plasma to pre-formed spike-ACE2 receptor complexes led to their dissociation. Finally, we observed that the RBD of HKU1, OC43, and SARS-CoV coronaviruses, but not unrelated control proteins, were able to compete substantially with the RBD of SARS-CoV-2 in solution. Therefore, the affinity of total plasma immunoglobulins to SARS-CoV-2 is an indicator of the quality of the immune response to SARS-CoV-2, and may help select the most efficacious samples for therapeutic plasmapheresis.

Introduction

The emerging severe-acute respiratory syndrome coronavirus 2 (SARS-CoV-2) pandemic has not only led to an enormous increase in mortality all over the world[2], but is also having a severe impact on and impairment of health-care systems, economic, and socio-economic indicators. Therefore, the rapid development of drugs and vaccines is of utmost importance to tackle the crisis. An understanding of the biochemical processes involved in the SARS-CoV-2 infection, particularly relating to the immune response, will be required to best design both treatments and vaccines. Adaptive humoral immune responses are crucial for defending hosts against incoming viruses[3]. However, the individual immune responses to any given virus are highly variable, and this can translate into different efficacies of viral clearance. Several studies have investigated antibodies generated during SARS-CoV-2 infection, thereby dissecting the antibody occurrence upon immune response[4-8], antibody cross-reactivity[9], disease prevalence in certain geographical areas[1,10,11], and the temporal evolution of the antibody response on the population level[1,10,11]. Furthermore, multiple ongoing studies focus on the applicability of antibodies for therapeutic purposes[12], including plasmapheresis[13-17], which may be a promising therapeutic strategy[17]. In such studies, occurrence of IgG antibodies has consistently been detected within two weeks after infection[1,4,6].

The biophysical parameters that govern the interaction between any antibody and its cognate antigen are its binding affinity and its concentration. Antibody titres are usually determined by enzyme-linked immunosorbent assay (ELISA) of serially-diluted samples, and represent a convolution of antibody affinity and concentration. Samples which contain low concentrations of high-affinity antibodies, and those with large amounts of low-affinity would exhibit identical immunological titres. These two scenarios may result in distinct biological properties which cannot be predicted by simple titration. While there have been efforts to infer antibody affinities through such approaches[18,19], these methods are often fraught with large error margins.

Here we determined affinity and concentration directly in plasma samples of seropositive individuals using Microfluidic Antibody Affinity Profiling (MAAP)[20]. We quantified both parameters in 39 seropositive individuals who presented either mild symptoms or were asymptomatic, demonstrating a comparable immune response which is independent of the symptoms displayed. By longitudinally monitoring antibody responses in severely symptomatic COVID-19 patients, we found an increase in antibody concentration, but no change in affinity, over the course of infection. In all samples with detectable binding, the binding affinity was stronger than the interaction between SARS-CoV-2 spike protein (S) and its associate receptor, the angiotensin converting enzyme 2 (ACE2), by which the virus infects host cells[21]. Our results are consistent with the idea that the immune response to SARS-CoV-

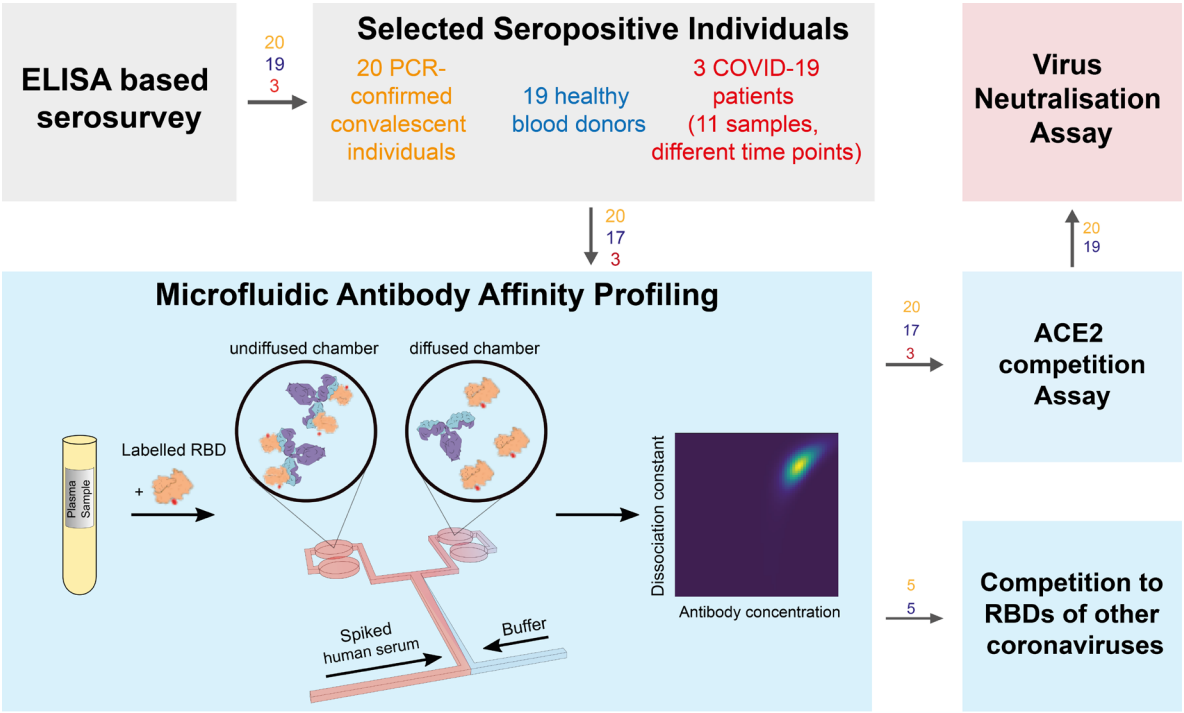

Figure 1: Principle of the study. First, we selected seropositive individuals based on a large-scale sero-survey[1] and performed four assays: Microfluidic Antibody Affinity Profiling (MAAP), cell-based plaque neutralisation assay, ACE2 competition assay and RBD cross-reactivity. For MAAP, blood is drawn from individuals who underwent an infection with SARS-CoV-2 as confirmed by ELISA, independent of symptoms they display. The blood cells are removed by centrifugation and fluorescently labelled RBD protein is added to the plasma, leading to complex formation between the antibodies abundant in the plasma and the extrinsically added fluorescently conjugated protein. The ACE2 competition assay and RBD cross-reactivity assay, which rely on co-incubation of the RBD with antibodies and a competitor molecule, show a decrease in hydrodynamic radius upon successful competition.

2 is predominately driven by inhibitory antibodies that effectively reduce the binding affinity of the target to the receptor.

Results and Discussion

Determination of Antibody Affinity and Concentration in Plasma. As part of a large-scale seroprevalence survey, plasma from over 10,000 healthy donors from the blood donation service (BDS) of the canton of Zurich was investigated for the presence of antibodies against SARS-CoV-2 Spike (S), receptor binding domain (RBD) and nucleocapsid proteins[1]. Seropositivity was defined as having a probability of being seropositive of ≥0.5, using our tripartite immunoassay[1]. To characterise the affinity-concentration relationship, we selected 19 healthy donors with sufficient residual plasma volume with a probability ≥0.85 to be seropositive, who were not diagnosed with SARS-CoV-2 previously. In addition, we investigated 20 PCR-confirmed convalescent individuals and three hospitalised patients with acute COVID-19 pneumonia, of which both cohorts were positive on ELISA as well (**Fig. 1**). The demographic characteristics of the seropositive collective are summarised in **Table S1**.

As an immune target, we selected the RBD of the spike protein, since it is crucial for antibody-dependent neutralisation by preventing host cell entry, and thus may be most significant in the immune response to SARS-CoV-2[22].

We determined the affinities and concentrations of RBD-reactive antibodies by measuring the equilibrium binding of antibodies in the plasma of seropositive individuals with the RBD directly in solution through MAAP, whereby the effective hydrodynamic radius of the Alexa647-labelled RBD protein was monitored. The measured radius increase upon complex formation with RBD-reactive antibodies allows detection and quantification of antibody binding (**Fig. 2**). Such measurements can be performed directly in plasma/serum, so that samples are not perturbed by additional purification procedures.

These binding measurements report on the combined response of all antibodies targeting different RBD epitopes at different affinities. In case there were multiple antibodies with different affinity present in the plasma sample, we are selective towards tighter binders (**Fig. S6**). First, we characterised the serum antibodies from 20 convalescent individuals and 17 healthy blood donors. 2 individuals could not be analysed on our platform due to presence of an excessively high serum background fluorescence, a known, yet rare, limitation of our assay[20]. A size increase, indicating significant binding to the RBD domain, was detected and quantified in all samples **(Fig. 2a**), with the exception of 6 healthy donor samples which we did not observe binding to the RBD domain by MAAP (**Fig. S2**). Considering all samples investigated, we found that the antibody concentration for the polyclonal antibody mixture falls into a relatively narrow range of 8-69 nM assuming a binding stoichiometry of 1:2 antibody:RBD, with two exceptions that display relatively high concentrations (192 nM and 298 nM). In contrast, the K_d values were more variable, ranging from subnanomolar (in which case no lower bound on K_d can be determined) to 25 nM (**Fig. 2b**). From physical considerations in order for significant binding to occur, the antibody binding site concentration must exceed the K_d. Accordingly, our data demonstrate that in all cases where quantifiable binding was detected, [Ab] > 2*K_d (**Fig. 2b**). Interestingly, also the 3 hospitalised patients displayed affinities and concentrations in a similar range, although their antibody concentration higher than the majority of samples (**Fig. 2b**). This suggest that the antibody response to a SARS-CoV-2 infection is fairly similar, independent of the symptoms displayed by an individual.

We next determined the dissociation constant for the interaction between spike protein and ACE2 receptor to be 30 nM (**Fig. S3**). This is higher than the K_d for almost all the plasma samples of the seropositive individuals. This indicates that, during the immune response, antibodies with higher affinity than the virus-receptor interaction are produced. Moreover, the relatively little excess in the concentration of antibody binding sites compared to K_d in most

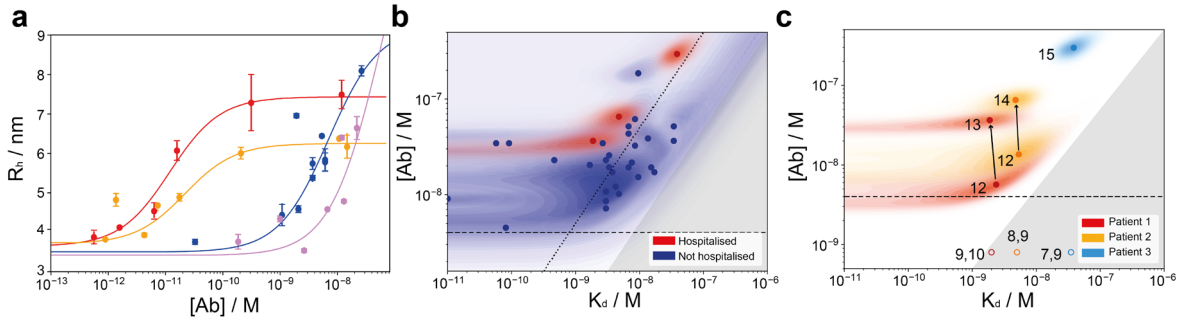

Figure 2: (**a**) Binding curves for four samples. Tight binders (red curve (K_d < 4.1·10^{-10} M) and maroon curve (K_d < 6.7·10^{-10} M)) are visibly distinguishable from weaker binders (blue curve (K_d = 8.5·10^{-9} M) and violet curve (K_d = 3.4·10^{-8} M)), as they reach the binding transition at earlier concentrations. As a mixture of differently glycosylated antibodies is investigated, different radii for the fully bound complex are observed for different individuals[1]. (**b**) Probability distributions of dissociation constants, K_d, and antibody concentrations, assuming two RBD binding sites per antibody, for seropositive individuals (blue) and hospitalised COVID-19 patients (red), where significant binding to the RBD was detected. Points correspond to the maximum probability values in the two-dimensional probability distribution, and shaded regions to the probability density. In line with physical principles of binding, binding is not observed for samples with [Ab] < 2K_d (dark grey region). Notably, some individuals express RBD-reactive antibody such that [Ab] ≥10 K_d (dotted line). (**c**) Time evolution of K_D and [Ab] probability distributions in patients who required hospitalisation. In both patients monitored during the infection (red and orange, filled circles), the antibody concentration increased over time, with no change in binding affinity. Numbered labels indicate the number of days post disease onset (DPO), while the grey area represents the region of parameter space which is inaccessible to MAAP. Open circles illustrate possible parameter values for earlier timepoints, for which binding was not detectable, and their position is randomised.

individuals may imply that affinity maturation is not continued beyond these minimum requirement, and only sufficient antibody is produced that to compete with the ACE2 to RBD interaction. Moreover, our binding equilibria are thus achieved under physiologically relevant conditions and our in-solution measurements allow to determine both the antibody affinity and concentration. As discussed previously[20], the commonly used EC50 values obtained through surface measurements may depend on both the antibody affinity and concentration. In contrast, MAAP allows simultaneous deconvolution of these two fundamental physico-chemical properties which describe antibody binding, a clear advantage over common surface-based techniques.

Affinity-Concentration Fingerprint at Early Time Point of Immune Response. To understand how affinity and concentration of the antibodies evolve over early timepoints, we investigated antibody maturation in three hospitalised COVID-19 patients. All three patients suffered from diabetes, with patients 2 and 3 presenting additional cardiovascular conditions, and requiring hospitalisation due to pneumonia. Analyses were performed for patient 1 (days post onset (DPO) 9 -13), patient 2 (DPO 8 -14), and patient 3 (DPO 7 -15). In all cases, no binding was detected until day 12 by MAAP, consistent with the ELISA data[1] and previous

literature[4,6]. Analysis of plasma samples taken from patients 1 and 2, taken one-two days apart, respectively, indicate that antibody concentration increases with no change in binding affinity (DPO 12 and 13 for patient 1, and DPO 12 and 14 for patient 2) (**Fig. 2c**). For patient three, only one time point could be effectively measured (**Fig. 2c**). These data, therefore, further support the hypothesis that, after producing an antibody with sufficiently high affinity, the affinity is not increased further, in favour of increasing antibody production. While our data are limited to just two timepoints in two patients, this effect is striking, and in contrast to previous work on Ebola, where antibody affinity has been found to increase as a function of time[23].

Neutralisation and ACE2-Receptor Binding Competition. From an immunological point of view, the interaction between the RBD region of the spike protein and the ACE2 receptor needs to be inhibited, mostly via antibodies that bind to the RBD. First, we investigated the degree of neutralisation on wildtype virus using a conventional virus neutralisation assay. From 37 seropositive individuals tested, 17 neutralisation activity when diluted 1:20 but no longer at 1:80, 10 had titres between 1:80 and 1:320 and 4 displayed titres < 1:320, while 6 did not show any neutralisation. (**Fig. 3a-b and Fig. S4**). The 6 samples which did not show neutralisation had relatively low titres against RBD on ELISA, and four of them did not show significant binding on the MAAP assay (**Table S2**). We then aimed to compare these results to the inhibitory effect of antibodies directed against the RBD of the spike protein using our microfluidics-based methodology. We therein incubated the samples of seropositive individuals, S1 and fluorescently-labelled ACE2 protein simultaneously (**Fig. 3c**). The observed hydrodynamic radius, R_h, of the ACE2 protein increases in the presence of S1 and seronegative plasma samples, as expected from binding of ACE2 to the S1 protein (**Fig. 3d**). However, upon the addition of seropositive plasma samples, this size increase is abrogated, indicating that the antibodies preventing binding of the S1 to ACE2 as such are inhibitory. This was observed for every sample for which we could determine a dissociation constant apart from one exception where we could determine a dissociation constant but did not observe neutralisation in the cell-based assay. The subsequent comparison of cell-based neutralisation with affinity and concentration show that the lowest concentration of antibody for which neutralisation is observed ranges between 80 pM to 2 nM, a relatively narrow range. Therefore, we hypothesise that two of the prerequisites for neutralisation are (a) an antibody concentration in the range between 80 pM to 2 nM and (b) an affinity of the RBD that is stronger for the antibody than for the ACE2 receptor (**Fig. 3 e-f**). This novel, microfluidic neutralisation surrogate is in good agreement with the cell-based neutralisation assays (**Fig. 3g** and **Table S2**).

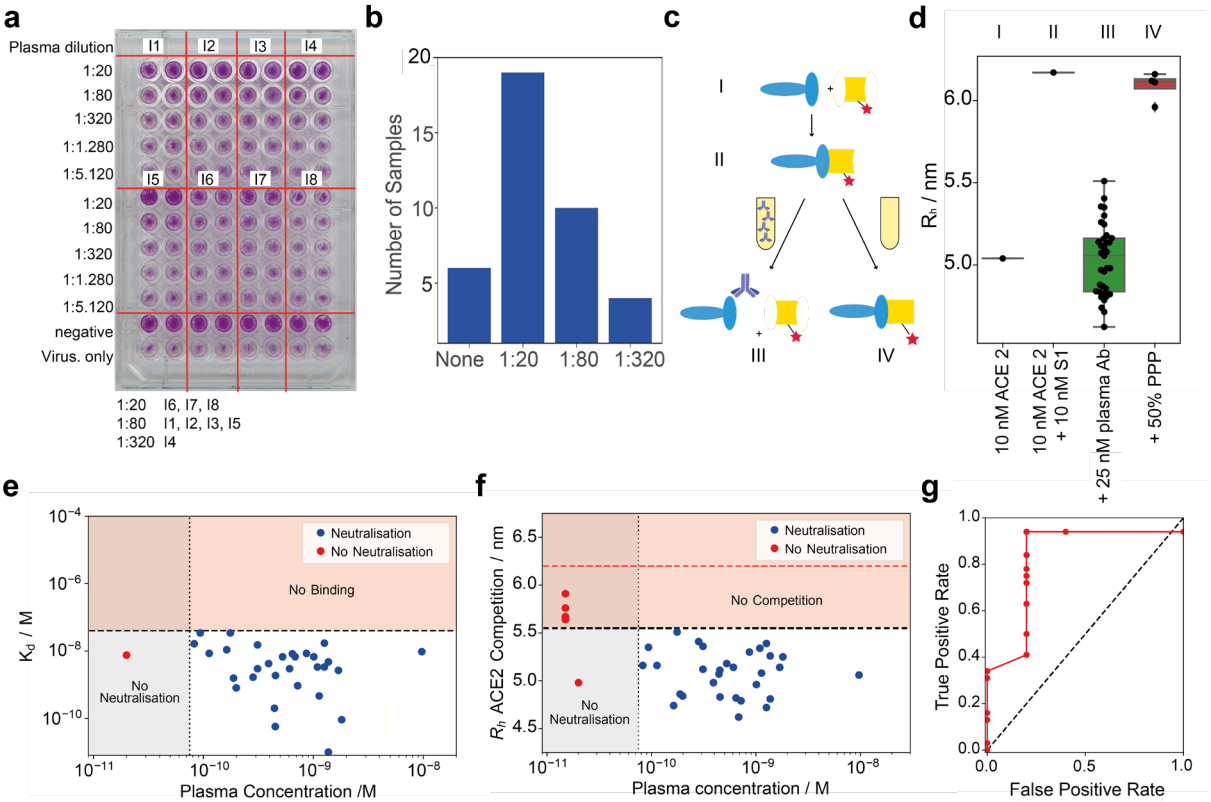

Figure 3: (**a**) Cell-based plaque neutralisation assay. Example plate. We observe neutralisastion at dilution 1:20 for blood samples from individuals 6, 7, and 8, 1:80 for individuals 1, 2, 3 and 5, and 1:320 for individual 4. All images shown in Fig. S4. (**b**) Cell-based plaque neutralisation assay. From 37 seropositive individuals tested, 6 showed no neutralisation, 19 showed a titer < 1:20, with 11 having titres between 1:80 and 1:320 and 4 having titres < 1:320. (**c**) Scheme of the competition assay. We incubate the spike protein with the ACE2 receptor, leading to a complex formation. Upon addition of plasma, this complex is disassembled. (**d**) Hydrodynamic radius of ACE2 in presence of spike protein in plasma of seropositive individual. When seropositive samples are used, no binding is detected, demonstrating the capability of the antibodies present in plasma to inhibit the interaction relevant for cellular uptake of the virus; in contrast, pre-pandemic plasma (PPP) samples do not inhibit the spike-ACE2 interaction. (**e**) Plot of the critical concentration at which neutralisation is observed vs. dissociation constant. We calculated this from the titers in the cell-plaque neutralisation assay and the concentrations determined in Fig. 2b. In order to be neutralising, the antibody needs to have an affinity tighter than the interaction to ACE2 (dashed horizontal line/orange region) and needs to lie in the concentration range 80 pM to 2 nM. Below this concentration, the amount of antibody does not enable neutralisation. Error bars omitted for visibility. The individual for whom no neutralisation is observable has an insufficiently high antibody concentration. The cut-off values were derived from the ROC curve Fig. 3g, with the optimal ratio between true positive and false positive. (**f**) Comparison between the hydrodynamic radius surrogate for neutralisation and the cell-based neutralisation data, with the same non-detectability regions and yielding a similar picture as Fig. 3e. As cut-off value, we used 5.5 nm, as shown in Fig. 3d and Fig. 3g. The red line represents the size of the bound complex. Error bars omitted for visibility. (**g**) ROC curve comparing the outcome of the microfluidic experiment with the cell-plaque based experiments. At a cut-off value of 5.5 nm (Fig. 3d).

Cross-Reactivity to other RBDs. Often discussed is a potential cross-reactivity of SARS-CoV-2 antibodies to RBD from related coronaviruses. We further investigated this cross-

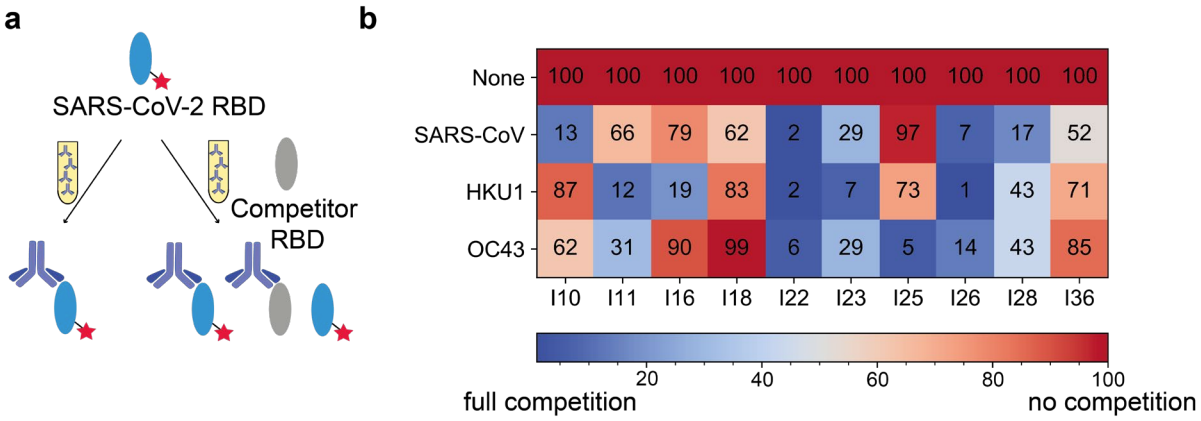

Figure 4: Cross Reactivity between different RBDs. (**a**) Assay principle. Labelled SARS-CoV-2 RBD is incubated against antibodies from plasma of seropositive individuals. In absence of any competing RBDs, the binding saturates. In presence of unlabeled competitor RBD, the antibodies can bind to both the labelled SARS-CoV-2 RBD and the unlabeled competitor RBD, which in turn causes unbound labelled RBD, causing a decrease in the apparent hydrodynamic radius of the mixture. (**b**) Relative decrease of hydrodynamic radii, in percent, for 10 individuals with different competitor RBDs of SARS-CoV, HKU1 and OC43. 0% indicates that there is no size increase as compared to pure SARS-CoV-2 RBD, meaning that binding of the antibodies to the SARS-CoV-2 RBD is fully inhibited, whilst 100% means no prevention of the binding, i.e. no competition.

reactivity of the antibodies for ten, randomly chosen, individuals from the previously tested cohort, 5 of which were healthy donors (I10, I11, I16, I18 and I36), and five of which were convalescent individuals (I22,I23,I25,I26,I28) (**Fig. 4** and **S5**). For this purpose, we incubated both labelled SARS-CoV-2 RBD and unlabelled RBD for other coronaviruses (SARS-CoV, HKU1 and OC43) with the plasma samples. If these RBDs are able to compete for binding, we would observe a decrease in hydrodynamic radius relative to the SARS-CoV-2 RBD measurement. For 5 individuals, most cross reactivity was observed for the SARS-CoV RBD, samples from two individuals showed most cross-reactivity was observed for RBD from OC43 and three samples for RBD from HKU1. Our data highlights that a potent immune response against one coronavirus can elicit cross-reactive antibodies against RBD domains of other coronaviruses. This finding may be crucial at identifying different SARS-CoV-2 strains that may be circulating in the future, as it becomes assumable that immunity from a pre-infection with one SARS-CoV-2 strain is protective against a different strand as well.

Conclusion

Antibody responses against a pathogen involve three critical features: The specific epitope that is targeted, antibody concentration, and the affinity of its interaction with the antigen. Here, we characterised the latter two for the RBD domain of the spike protein, using Microfluidic Antibody Affinity Profiling, directly in solution. We have observed that the net antibody concentration is fairly uniform across different individuals with varying symptom severity (8-69

nM), while a higher variability in K_d is observed, ranging from sub-nanomolar to tens of nanomolar. However, in all cases where binding in plasma was significant enough to be quantified (i.e. where [Ab] > $2K_d$), this interaction was strong enough to prevent the interaction between the ACE2 receptor and the spike protein. This finding was confirmed with a virus-based plaque neutralisation assay, where all samples, but one, which were able to out-compete ACE2 binding *in vitro* showed neutralisation *in vivo* as well. Lastly, we identified that the immune response against SARS-CoV-2 holds the potential to recognise RBD epitopes from other coronaviruses, suggesting that antibodies capable of neutralisation may be produced by activated memory B cells even when triggered by an alternative future SARS-CoV-2 variant.

The relationship between antibody concentration and affinity is likely to have consequences for plasmapheresis, together with targeting the appropriate epitopes for efficient neutralisation. During plasmapheresis treatment, the donor plasma is diluted by roughly a factor of ten upon transfusion into the patient[17]. For the donor antibodies to still bind viral proteins effectively following this dilution, in the case where the patient has produced no antibodies, the antibody binding site concentration should thus exceed the K_d by at least a factor of ten. We hypothesise that the success of plasmapheresis is dependent on the ratio of [Ab]/K_d of the neutralising fraction of antibodies. Therefore, only the patients with very strong K_d values should be considered as blood donors for plasmapheresis, a parameter that cannot be sufficiently accessed with conventional methods.

Methods

Ethical and biosafety statement. All experiments and analyses involving samples from human donors were conducted with the approval of the local ethics committee (KEK-ZH-Nr. 2015-0561, BASEC-Nr. 2018-01042, and BASEC-Nr. 2020-01731), in accordance with the provisions of the Declaration of Helsinki and the Good Clinical Practice guidelines of the International Conference on Harmonisation.

Sample Collection. EDTA plasma from healthy donors and from convalescent individuals was obtained from the Blutspendedienst (blood donation service) Kanton Zürich from donors who signed the consent that their samples can be used for conducting research. Samples from patients with COVID-19 were collected at the University Hospital Zurich from patients who signed an informed consent.

Reagents. SARS-CoV-2 RBD, ACE2-receptor protein and SARS-CoV-2 spike S1 protein were purchased from SinoBio (Eschborn, DE). RBDs from SARS-CoV, HKU1, and OC43 were purified as outlined[1]. Microfluidic chips and cartridges for the measurements performed on the Fluidity One-W platform were provided by Fluidic Analytics (Cambridge, UK).

Labelling. SARS-CoV-2 RBD and ACE2 receptor protein were labelled using amine coupling based on NHS chemistry with AlexaFluor 647 dye. To RBD (typically 1 nmol, 1 equiv.) in 0.1 M $NaHCO_3$ (pH = 8), Alexa Fluor 647 *N*-hydroxysuccinimide ester (in DMSO, 3 equiv.) was added. The reaction mixture was incubated for overnight at 4 °C, protected from light. The sample was purified by size exclusion chromatography (Superdex 200 increase) with a flow rate of 0.05 mL/min and PBS as eluent buffer, to yield labelled protein.

Affinity and Concentration Determination. Microfluidic Antibody Affinity Profiling measurements were performed as reported previously[20]. For the MAAP measurements, varying fractions of human plasma samples were added to a solution of the antigen of concentrations varying between 10 nM and 150 nM, and PBS (containing 0.05 % Tween 20, SA) was added to give a constant volume of 20 µL. The antigen used was RBD labelled with Alexa Fluor 647 through N-terminal amine coupling. These samples were incubated at room temperature for 40 minutes and the size of the formed immunocomplex was determined through measuring the hydrodynamic radius, R_h, with microfluidic diffusional sizing using the Fluidity One-W platform. In order to determine the dissociation constant, K_d = [Ab][R]/[AbR], where [Ab] and [R] are the equilibrium concentrations of antibody binding sites and RBD domain, respectively, and [AbR] is the concentration of bound RBD. The data were analysed by Bayesian inference, according to the following equations. Following correction of fluorescence intensities for plasma autofluorescence, the fraction, f_d, of RBD to diffuse into the distal channel is defined by[24]

$$f_d = \frac{[AbR](1-\rho_b) + ([R]_0 - [AbR](1-\rho_f))}{[R]_0}$$

where $[R]_0$ is the total concentration of RBD, and ρ_b and ρ_f are the fractions of bound and free RBD to diffuse into the distal channel, respectively. By solving the binding equation, we obtain the following expression for [AbR]

$$[AbR] = \frac{\alpha[Ab]_{tot} + [R]_0 + K_D - \sqrt{(\alpha[Ab]_{tot} + [R]_0 + K_D)^2 - 4\alpha[Ab]_{tot}[R]_0}}{2}$$

where α is the fraction of plasma used in the measurement and $[Ab]_{tot}$ is the total concentration of antibody binding sites in the sample. K_d and $[Ab]_{tot}$ were thus determined through Bayesian inference, with ρ_b and ρ_f as additional parameters to be inferred. The prior was considered to be flat in logarithmic space for K_d and $[Ab]_{tot}$, flat in linear space for ρ_b, and normally distributed in linear space for ρ_f (using μ and σ determined through measurements of the purified RBD). The likelihood function was considered to be Gaussian, with a standard deviation obtained through replicate measurements.

ACE2 Competition. S1 protein (10 nM) and ACE2 receptor protein (10 nM) were incubated in PBS for approx. 40 minutes. Subsequently, antibody in seropositive plasma was added to the mixture to a final antibody concentration of 25 nM and incubated for approx. 1 h. The hydrodynamic radius was determined by microfluidic diffusional sizing (Fluidity One-W, Fluidic Analytics, Cambridge UK).

RBD Cross-Reactivity Competition. Labelled SARS-CoV-2 RBD (10 nM) and was incubated against antibody in a plasma sample, for a final antibody concentration of 25 nM and incubated for approx. 1 h. Subsequently, an unlabelled competitor RBD was added (10 nM) The hydrodynamic radius was determined by microfluidic diffusional sizing (Fluidity One-W, Fluidic Analytics, Cambridge UK).

Virus Neutralisation Assay. The day before infection, VeroE6 cells were seeded in 96-well plates at a density of 12500 cells per well. Heat inactivated plasma samples from seropositive individuals were diluted 1:20 in DMEM 2% FCS in a separate 96-well plate. Four-fold dilutions were then prepared until 1:5120 in DMEM 2% FCS in a final volume of 60 µl. SARS-CoV-2 viral stock ($2.4x10^{-6}$ PFU/ml) diluted 1:100 in DMEM 2% FCS was added to the diluted sera at a 1:1 volume/volume ratio. The virus-plasma mixture was incubated at 37°C for 1 h. Then 100 µl of the mixture was subsequently added to the VeroE6 cells in duplicates. After 48h of incubation at 37°C cells were washed once with PBS and fixed with 4% fresh formaldehyde solution for 30 min at RT. Cells were washed once with PBS and plates were put at 58°C for 30 min before staining with 50 µl of 0.1% crystal violet solution for 20 min at RT. Wells were washed twice with water and plates were dried for scanning. A negative pool of sera from pre-pandemic healthy donors was used as negative control. Wells with virus only were used as positive controls.

References

1 Emmenegger, M. *et al.* Early plateau of SARS-CoV-2 seroprevalence identified by tripartite immunoassay in a large population. *medRxiv*, 2020.2005.2031.20118554, doi:10.1101/2020.05.31.20118554 (2020).
2 World Health Organisation. Coronavirus Disease (COVID-19) Weekly Eidemiological Update 1. (Geneva, 2020).
3 Beutler, B. Innate immunity: an overview. *Mol. Immunol.* **40**, 845-859 (2004).
4 Long, Q.-X. *et al.* Antibody responses to SARS-CoV-2 in patients with COVID-19. *Nat. Med.* **26**, 845-848 (2020).
5 Xiang, F. *et al.* Antibody Detection and Dynamic Characteristics in Patients with COVID-19. *Clin. Infect. Dis.*, doi:10.1093/cid/ciaa461 (2020).
6 Guo, L. *et al.* Profiling Early Humoral Response to Diagnose Novel Coronavirus Disease (COVID-19). *Clin. Infect. Dis.* **71**, 778-785 (2020).
7 Du, Z., Zhu, F., Guo, F., Yang, B. & Wang, T. Detection of antibodies against SARS-CoV-2 in patients with COVID-19. *J. Med. Virol.*, doi:10.1002/jmv.25820 (2020).
8 Okba, N. M. A. *et al.* SARS-CoV-2 specific antibody responses in COVID-19 patients. *medRxiv*, 2020.2003.2018.20038059, doi:10.1101/2020.03.18.20038059 (2020).
9 Tetro, J. A. Is COVID-19 receiving ADE from other coronaviruses? *Microb. Infect.* **22**, 72-73 (2020).
10 Abbasi, J. The Promise and Peril of Antibody Testing for COVID-19. *JAMA* **323**, 1881-1883 (2020).
11 Bendavid, E. *et al.* COVID-19 Antibody Seroprevalence in Santa Clara County, California. *medRxiv*, 2020.2004.2014.20062463, doi:10.1101/2020.04.14.20062463 (2020).
12 Jacobs, J. J. L. Neutralizing antibodies mediate virus-immune pathology of COVID-19. *Med. Hypotheses* **143**, 109884 (2020).
13 Chen, L., Xiong, J., Bao, L. & Shi, Y. Convalescent plasma as a potential therapy for COVID-19. *The Lancet Infectious Diseases* **20**, 398-400 (2020).
14 Perotti, C. *et al.* Plasma from donors recovered from the new Coronavirus 2019 as therapy for critical patients with COVID-19 (COVID-19 plasma study): a multicentre study protocol. *Intern. Emerg. Med.* (2020).
15 Seghatchian, J. & Lanza, F. Convalescent plasma, an apheresis research project targeting and motivating the fully recovered COVID 19 patients: A rousing message of clinical benefit to both donors and recipients alike. *Transfusion and Apheresis Science*, doi:10.1016/j.transci.2020.102792 (2020).
16 Casadevall, A. & Pirofski, L.-a. The convalescent sera option for containing COVID-19. *The Journal of Clinical Investigation* **130**, 1545-1548 (2020).
17 Zhang, L. *et al.* Anti-SARS-CoV-2 virus antibody levels in convalescent plasma of six donors who have recovered from COVID-19. *Aging* **12**, 6536-6542 (2020).
18 Chiem, N. H. & Harrison, D. J. Monoclonal antibody binding affinity determined by microchip-based capillary electrophoresis. *Electrophoresis* **19**, 3040-3044, doi:10.1002/elps.1150191641 (1998).
19 Hollemans, H. J. G. & Bertina, R. M. Scatchard Plot and Heterogeneity in Binding Affinity of Labeled and Unlabeled Ligand. *Clin. Chem.* **21**, 1769-1773, doi:10.1093/clinchem/21.12.1769 (1975).
20 Schneider, M. M. *et al.* Microfluidic Antibody Affinity Profiling for In-Solution Characterisation of Alloantibody - HLA Interactions in Human Serum. *bioRxiv*, 2020.2009.2014.296442, doi:10.1101/2020.09.14.296442 (2020).
21 Varga, Z. *et al.* Endothelial cell infection and endotheliitis in COVID-19. *The Lancet* **395**, 1417-1418 (2020).
22 Wang, X. *et al.* Neutralizing Antibody Responses to Severe Acute Respiratory Syndrome Coronavirus 2 in Coronavirus Disease 2019 Inpatients and Convalescent Patients. *Clin. Infect. Dis.*, doi:10.1093/cid/ciaa721 (2020).

23 Khurana, S. *et al.* Longitudinal Human Antibody Repertoire against Complete Viral Proteome from Ebola Virus Survivor Reveals Protective Sites for Vaccine Design. *Cell Host Microbe* **27**, 262-276.e264 (2020).
24 Linse, S. *et al.* Kinetic fingerprints differentiate anti-Aβ therapies. *bioRxiv*, 815308, doi:10.1101/815308 (2020).

Acknowledgements

All authors wish to thank their entire teams for support in the lab. We thank Tom Scheidt (IMB, Mainz) who provided graphics for **Figure 1**. We are grateful to Aaron Ring, John D. Huck, and Feimei Liu (Yale School for Medicine) for sharing the SARS-CoV, HKU1, and OC43 RBD proteins. Blood of COVID-19 patients from the USZ was acquired with the help of Irina L. Dubach and Dominik I. Schaer, whom we kindly acknowledge. We are grateful to all blood donors and hospital patients for helping us conduct this study.

Funding

We acknowledge financial support from the BBRSC to TPJK, as well as the Frances and Augustus Newman Foundation to TPJK; the ERC PhyProt (agreement no. 337969) to MMS, CKX, MRZ, GM and TPJK; the Centre for Misfolding Diseases, Cambridge to MMS, CKX, GM, and TPJK; St John's College Cambridge to MMS, MRZ and TPJK; as well as CKX and MRZ from the Herchel Smith Fund; ICM acknowledges funding from the Swiss FCS. Institutional core funding by the University of Zurich and the University Hospital of Zurich to AA, as well as Driver Grant 2017DRI17 of the Swiss Personalized Health Network to AA; Funding by grants of Innovation Fund of the University Hospital Zurich to AA and ME. VK acknowledges funding from NIHR (PDF-2016-09-065).

Competing interests

TPJK is a member of the board of directors of Fluidic Analytics. AA is a member of the board of directors of Mabylon AG which has funded antibody-related work in the Aguzzi lab in the past. VD, SF, HF are employees of Fluidic Analytics. All other authors declare no competing interests.

Author contribution

Performed the microfluidic measurements and analysed data: MMS, CKX, ICM, SF, GM, MRZ, TPJK, AA. Performed the plaque neutralisation assay and analysed data: PT, DT. Performed the labelling of antigens: VD, SF, HF. Designed study: MMS, ME, ICM, VK, HF, DT, TPJK, AA. Coordinated and collected the samples for this study: BMF, ME. Advised on experiments: ME, TPJK, AA. Wrote the manuscript: MMS, ME, CKX, ICM, TPJK, AA. Supervised the study: AA, TPJK, DT.

Data availability

The raw data underlying this study will be made available upon reasonable request. The biobank samples are limited and were exhausted in several instances. Therefore, while we will make efforts to provide microliter amounts of samples to other researchers, their availability is physically limited.